Developmental Biology 328 (2009) 506–516

Contents lists available at ScienceDirect

Developmental Biology

journal homepage: www.elsevier.com/developmentalbiology

A SHH-independent regulation of Gli3 is a significant determinant of anteroposterior patterning of the limb bud

Patrick Hill, Katrin Götz, Ulrich Rüther *

Institut für Entwicklungs- und Molekularbiologie der Tiere, Heinrich-Heine-Universität Düsseldorf, 40225 Düsseldorf, Germany

ARTICLE INFO

Article history:
Received for publication 27 June 2008
Revised 27 January 2009
Accepted 13 February 2009
Available online 24 February 2009

Keywords:
GLI3 repressor
Sonic hedgehog
Polarity
Digit identity
Limb development

ABSTRACT

The family of GLI proteins (GLI1–3) comprises the intracellular mediators of the hedgehog pathway, which regulates a myriad of developmental processes, one of which is limb development. Whereas GLI1 and GLI2 seem to be dispensable during limb development, GLI3 is especially crucial since all GLI3-associated human congenital diseases comprise limb malformations. Furthermore, *Gli3*$^{-/-}$ mouse embryos exhibit pronounced polydactyly in conjunction with a loss of digit identities.

Here we examined how the quantity of GLI3 contributes to its function by using different *Gli3* mutants in order to vary overall GLI3 levels. In addition, we made use of the *Gli3*$^{\Delta 699}$ allele, which encodes a C-terminally truncated version of GLI3, thus mimicking the processed GLI3 isoform (GLI3R). The *Gli3*$^{\Delta 699}$ mutant made it feasible to analyze isoform-specific contributions of GLI3 within the context of anteroposterior patterning of the limb bud. We revealed a so far unappreciated variation in the quantitative demand for GLI3 within different phases and aspects of distal limb formation. In addition, our analyses provide evidence that unprocessed full-length GLI3 is dispensable for anteroposterior patterning of the limb bud. Instead, digit identities are most likely defined by GLI3 repressor activity alone. Furthermore, we present evidence that the anteroposterior grading of GLI3 activity by the action of SHH is supported by a prototype patterning, which regulates *Gli3* independently from SHH.

Introduction

Mutations in *GLI3* manifest in at least five distinct clinical phenotypes, all of which include deformation of the limbs. Thus, the study of limb development has been a favourite model system to analyze the function of the GLI3 transcription factor. The GLI family (GLI1–3) comprises the vertebrate orthologues of *Drosophila* cubitus interruptus (ci). Ci is a bifunctional mediator of all extracellular hedgehog (hh) signals. In the absence of hh signaling, ci is processed to a truncated isoform that represses hedgehog target genes. Upon binding of hh to its receptor patched (ptc), processing of ci is prevented and the full-length isoform serves as a transcriptional activator of hh target genes (Aza-Blanc et al., 1997; Ohlmeyer and Kalderon, 1998; Aza-Blanc and Kornberg, 1999; Wang and Holmgren, 1999). In vertebrates, the members of the GLI family are the mediators of Sonic hedgehog (SHH) signaling (reviewed in Ingham and McMahon, 2001; Cohen, 2003).

A number of severe diseases in humans are caused by mutations within the Hedgehog signaling pathway (Nieuwenhuis and Hui, 2005). While GLI1 is of major medical significance because of its role in tumorigenesis (reviewed in Kasper et al., 2006), GLI3 is very important for embryonic development. Mutations in *GLI3* cause several congenital diseases including Greig cephalopolysyndactyly syndrome (GCPS) and Pallister–Hall syndrome (PHS) (Vortkamp et al., 1991; Kang et al., 1997; Wild et al., 1997). Most of the clinical characteristics of *GLI3* associated syndromes are distinct, but all share digit abnormalities. Only GLI3 seems to exert such an irreplaceable function in limb development since GLI1 and GLI2 deficient mouse embryos develop well patterned extremeties (Park et al., 2000; Bai et al., 2002). The effects of a loss of GLI3 function can be seen in *extra-toes* (*XtJ*) mice, which carry a *Gli3* null allele and represent a mouse model for GCPS (Hui and Joyner, 1993; Büscher et al., 1998). Heterozygous *Gli3*$^{+/-}$ mice display mild preaxial polydactyly (= supernumary digits at the anterior side) while the limbs of homozygous *Gli3*$^{-/-}$ embryos exhibit severe polydactyly associated with a complete loss of digit identities (Hui and Joyner, 1993). Consequently, GLI3 is believed to act in the regulation of both the number and the identity of digits. Inevitably, the difference between heterozygous and homozygous *Gli3*$^{-}$ embryos points to the fact, that the quantity of GLI3 is an important issue. However, as yet, we still do not have a clear picture in how far the quantity of GLI3 contributes to the establishment of the different parameters of normal limb development. Furthermore, different studies suggest that GLI3 may function as both an activator and repressor of Sonic Hedgehog (SHH) signaling (Dai et al., 1999; Sasaki et al., 1999; Motoyama et al., 2003). Like cubitus interruptus, full-length GLI3 (GLI3-FL) is processed to form a shorter isoform (GLI3 repressor; GLI3R) in the absence of SHH signaling (Wang et al., 2000; Litingtung et al., 2002). Complete deprivation of SHH

* Corresponding author. Fax: +49 1 211 81 15113.
E-mail address: ruether@uni-duesseldorf.de (U. Rüther).

0012-1606/$ – see front matter © 2009 Elsevier Inc. All rights reserved.
doi:10.1016/j.ydbio.2009.02.017

function in the $Shh^{-/-}$ mutant mouse results in defective development of many embryonic structures, including the limb. $Shh^{-/-}$ limbs have severe anteroposterior skeletal deficiencies distal to the stylopod/zeugopod junction (elbow/knee joints); all zeugopod and autopod elements are either missing, fused or lack normal identity, except for a single digit 1 in the hindlimb (Chiang et al., 2001; Litingtung et al., 2002). Recent results suggested that SHH function in limb development is largely confined to the regulation of GLI3 processing; thereby creating an anteroposterior GLI3-FL:GLI3R gradient, which has been proposed to regulate digit number and identity (Wang et al., 2000; Litingtung et al., 2002, te Welscher et al., 2002b; Wang et al., 2007). The loss of digits in the $Shh^{-/-}$ mutant has therefore been explained by an excess of the GLI3R isoform. However, $Shh^{-/-}$ mice are largely inapt to assess the contribution of GLI3 to the specification of digit identities because of the extensive loss of distal limb elements in the *Shh* mutant.

These downsides can now be avoided by the use of the $Gli3^{\Delta 699}$ mouse mutant (Böse et al., 2002). These mutant mice, which serve as a mouse model for the Pallister–Hall syndrom, carry a truncating mutation just 3′ of the sequences encoding the DNA-binding domain of GLI3 (Böse et al., 2002). The molecular size of the $GLI3^{\Delta 699}$ protein is very similar to the endogenously produced wild type GLI3R isoform and the protein expression level of $GLI3^{\Delta 699}$ parallels that of wild type GLI3 (Hill et al., 2007). The embryos exhibit anterior transformation of digit identities and the formation of posterior digits is compromised (Hill et al., 2007). Thus, within the context of anteroposterior (A/P) patterning of the limb bud $GLI3^{\Delta 699}$ executes all the functions, which have so far been proposed for GLI3R. However, $Gli3^{\Delta 699/\Delta 699}$ mutant embryos do not display the extensive loss of distal limb elements that is seen in $Shh^{-/-}$ mutants (Hill et al., 2007). Instead, digit number of $Gli3^{\Delta 699/\Delta 699}$ mutant embryos is within the normal range with a tendency towards polydactyly in the forelimb (Hill et al., 2007). Thus, $Gli3^{\Delta 699}$ mutants provide an excellent setting to study the isoform-specific contributions of GLI3 to A/P patterning during normal limb development. Furthermore, the $Gli3^{\Delta 699}$ mutation uncouples GLI3R repressor function from the posttranslational regulation by SHH.

Here, we used the $Gli3^{\Delta 699}$ and additional mouse mutants to manipulate both GLI3 levels and isoform ratios in order to assess the consequences on limb development. We could show how varying quantities of GLI3 selectively affect different aspects of limb development. Our results also indicate that previously identified functions of GLI3 seem to be mediated largely if not solely by the GLI3 repressor isoform. Therefore, our analysis challenges previous interpretations, which stated that both isoforms contributed actively to the appropriate anteroposterior patterning of the limb bud. In addition, our results uncover the so far neglected importance of a SHH-independent A/P patterning for the proper regulation of *Gli3*.

Materials and methods

Bone and cartilage staining

Embryos were fixed in 80% ethanol, skinned and eviscerated. Subsequently they were dehydrated in ethanol overnight, degreased in acetone overnight, and stained in Alcian blue/Alizarin Red overnight at 37 °C. Embryos were then rinsed with ethanol for 1 h, and finally were run through an 1% potassium hydroxide: glycerol series and stored in pure glycerol. In line with classical definitions we indicated the bones of feet as autopod (autopodial), bones directly proximal to the toes (digits) as metapodial and ulna/radius (tibia/fibula) as zeugopod.

WISH

Whole-mount in situ hybridizations were performed essentially as described previously (Grotewold et al., 1999). Probe information can be provided on request.

Mice

$Gli3^{\Delta 699}$, $Gli3^{Pdn}$ and $Gli3^{Xtj}$ mice were maintained as heterozygous stocks in a mixed C57BL/6×C3H background. Heterozygous $Gli3^{\Delta 699}$ mice were crossed to $Gli3^{Xtj}$ and $Gli3^{Pdn}$ heterozygous mice to generate *Gli3* double heterozygous mutant embryos. Embryonic day 0.5 was the day vaginal plugs were found. Embryos were harvested between E10.5 and E19.5, and genotyping was performed on yolk sac DNA by Polymerase Chain Reaction (PCR). Primer information can be provided on request.

Results

Bone morphogenesis, digit number and digit identity are differentially regulated by GLI3 levels

The phenotypic difference between homozygous and heterozygous *Gli3* null mutants prompted us to analyze the quantitative requirement for GLI3 in detail. In order to broaden the available scale of different GLI3 levels, we also used a hypomorphic *Gli3* mutant, called *Polydactyly Nagoya* (*Pdn*). Previous analyses have shown, that $Gli3^{Pdn/Pdn}$ homozygotes produce 20–30% of the wild type mRNA level (Thien and Rüther, 1999; Ueta et al., 2004).

The distal extremities of wild type mice are arranged in an asymmetric way such that the anterior-most digit is short and comprises two bony segments, which are called phalanges (Figs. 1E, J, O). The four posterior digits are longer and triphalangeal (Figs. 1E, J, O). The phenotype of $Gli3^{-/-}$ mutants reveals very obviously that GLI3 is involved in the regulation of digit number and A/P asymmetry (Litingtung et al., 2002; te Welscher et al., 2002b). However, less attention has been given to additional consequences of the loss of GLI3. In our hands, $Gli3^{-/-}$ embryos developed 7–8 digits (Figs. 1A, F, K), which showed no prominent difference in length on the level of metapodial elements or between individual digits. In addition, the formation of proximal phalanges was heavily impaired. The region between the seemingly unaffected digit tips and the metapodial elements (metacarpals, metatarsals) commonly contained a single chondrogenic element in $Gli3^{-/-}$ embryos (Figs. 1F, K). This element lacked a proper articulation to its adjoining metacarpal or -tarsal. Instead it produced two proximal extensions. In the case of many $Gli3^{-/-}$ autopods, this situation changed gradually towards the posterior margin. The more posterior a digit the larger the misshapen single phalangeal element became. This continued up to the point where a triphalangeal digit formed at the posterior margin of the $Gli3^{-/-}$ autopod (Figs. 1F, K).

The external appearance of the limbs of $Gli3^{Pdn/-}$ embryos was in many aspects similar to that of $Gli3^{-/-}$ embryos. The paw was polydactylous with a nearly semicircular outline lacking the normal wild type asymmetry (Fig. 1B). Accordingly, skeletal stainings revealed no apparent divergence in the length of anterior vs. more posterior metapodial and digital elements (Figs. 1G, L). In contrast to $Gli3^{-/-}$, however, $Gli3^{Pdn/-}$ embryos developed digits with well-defined phalanges and intermediate joints. There was no large gap between the proximal phalanx and its adjoining metacarpal (-tarsal) (Figs. 1G, L). Still, 70% of fore- and hindlimbs in $Gli3^{Pdn/-}$ mutants lacked an anterior biphalangeal digit (Figs. 1G, L).

The extent of polydactyly in $Gli3^{Pdn/Pdn}$ embryos was similar to that of $Gli3^{-/-}$ and $Gli3^{Pdn/-}$ embryos (Figs. 1C, H, M; Table 1). However, along with increasing GLI3 levels, a further improvement of anterior–posterior patterning was apparent. In general, forelimbs of $Gli3^{Pdn/Pdn}$ embryos developed preaxial biphalangeal digits (Fig. 1H). Still, the anterior-most digit was clearly elongated compared to the wild type shape (Figs. 1C, H). This fact indicated that the parameters of normal anterior character were not completely established in $Gli3^{Pdn/Pdn}$ embryos. Rather remarkably, for the first time in our setting, polydactyly was significantly reduced in heterozygous $Gli3^{+/-}$

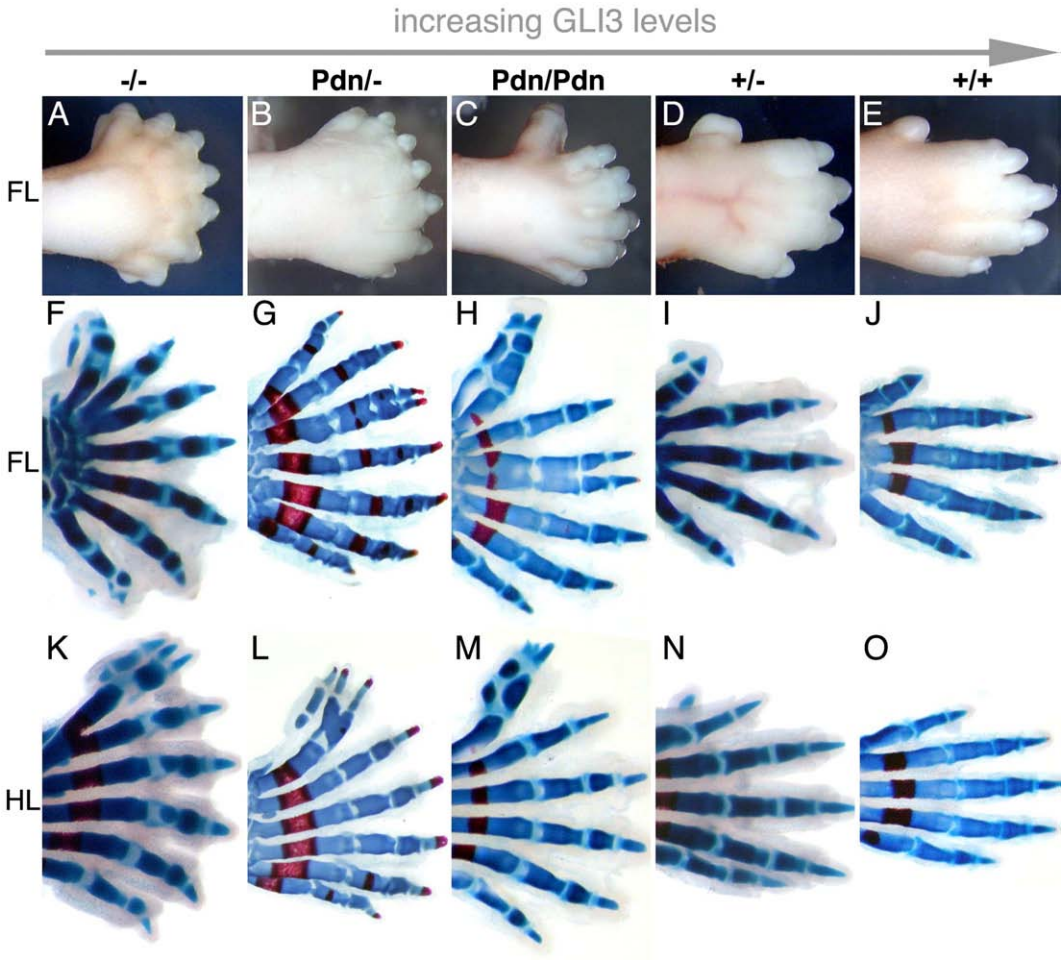

Fig. 1. Separate parameters of normal limb development show diverse sensitivity for a reduction in GLI3 levels. Dorsal view of untreated fore paws (A–E) and Alcian Blue/Alizarin Red stained fore- (FL) and hindpaws (HL) (F–O). Bone material is red, cartilage is blue. Anterior is upwards and distal is towards the right. (A, F, K) *Gli3*$^{-/-}$ embryos developed 7–8 digits lacking normal A/P asymmetry. Formation of the proximal phalanges was impaired. Generally, this failure improved gradually towards the posterior margin where a triphalangeal digit formed. (B, G, L) The paw of *Gli3*$^{Pdn/-}$ embryos was symmetrical and polydactylous. Skeletal stainings revealed intact phalangeal segmentation. Usually, the anterior digit was triphalangeal. (C, H, M) The polydactylous paws of *Gli3*$^{Pdn/Pdn}$ embryos were asymmetrical. The anterior-most digit of the forelimb was mostly biphalangeal but was abnormally elongated. (D, I, N) Heterozygous *Gli3*$^{+/-}$ embryos exhibited a normal A/P asymmetry and mild polydactyly. (E, J, O) *Gli3*$^{+/+}$ embryos develop the normal asymmetric autopod, which consists of a short anterior biphalangeal digit and four posterior triphalangeal digits.

embryos. They displayed relatively mild anterior polydactyly of the fore- and hindlimb (Figs. 1D, I, N). In the forelimb this included distal bifurcations of digit 2 in some cases (data not shown, Table 1). We never found any duplication of metapodial elements in *Gli3*$^{+/-}$ embryos (Table 1). Anteroposterior asymmetry was obvious as the anterior digit was always biphalangeal and clearly shorter than the more posterior ones (Figs. 1I, N). Heterozygous *Gli3*$^{Pdn/+}$ embryos exhibited an extremely mild polydactyly. Usually, they developed a small preaxial protrusion only in the hindlimb. Bone and cartilage stainings revealed none or at most a single minute cartilage element within that ectopic structure (data not shown).

Our comparison of different GLI3 quantities shows that several aspects of normal limb development are differentially susceptible to changes in GLI3 levels.

Table 1
Recordal of proximal and distal digital elements in *Gli3* mutants

		−/−	*Pdn*/−	*Pdn*/*Pdn*	+/−	*Pdn*/+	*Δ699*/−	*Δ699*/*Δ699*
Forelimb	Tips	**7.5**	**7.5**	**7.6**	**6.2**	**5**	**8**	**5.8**
	Min.–max.	6–9	7–8	7–8	5–7	5	6–9	4–7
	Metacarpals	**6.5**	**7.1**	**7.5**	**5**	**5**	**6**	**5**
	Min.–max.	6–7	7–8	7–8	5	5	6–7	4–6
Hindlimb	Tips	**7**	**7.1**	**7**	**6**	**5**	**6.6**	**5**
	Min.–max.	6–9	6–8	7–8	5–6	5–6	6–8	4–6
	Metatarsals	**5.8**	**6.2**	**6**	**5**	**5**	**6**	**4.8**
	Min.–max.	5–7	5–7	6	5	5	6–7	4–6
Number of specimen		9	11	3	19	18	18	5

Bold numerals show average quantities. Slim numbers represent the minimum and maximum values of the phenotypic spectrum within our assessment.

GLI3$^{\Delta 699}$ *is sufficient to specifiy anteroposterior digit identities*

One of the open questions concerning GLI3 function is whether both isoforms are required for the anteroposterior patterning of the limb bud, i.e. for the specification of digit identities. The use of *Gli3*$^{\Delta 699}$ mutants gives valuable insight into this matter because they specifically lack the GLI3-FL isoform and only produce a truncated GLI3 protein that is very similar to the processed short GLI3R isoform. Furthermore, GLI3$^{\Delta 699}$ has been shown to indeed exert GLI3 repressor function regarding the specification of digit identities (Hill et al., 2007).

Heterozygous *Gli3*$^{\Delta 699/+}$ embryos display well patterned limbs, which are phenotypically indistinguishable from those of wild type specimen (Figs. 2A, D, G). As discussed previously (Hill et al., 2007), homozygous *Gli3*$^{\Delta 699}$ mutants usually display a mild polydactyly in the forelimb but they may also show oligodactyly (Figs. 2C, F and data not shown; Hill et al., 2007). Both fore- and hindlimbs are characterized by anterior transformation of the digits, which is

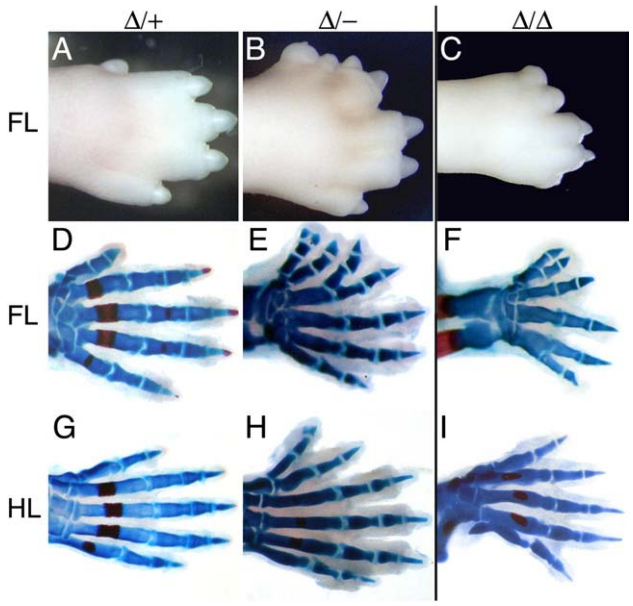

Fig. 2. Specification of digit identities by GLI3$^{\Delta 699}$. Dorsal view of untreated fore paws (A–C) and Alcian Blue/Alizarin Red stained fore (FL) and hind (HL) paws (D–I). Anterior is upwards and distal is towards the right. (A, D, G) *Gli3*$^{\Delta 699/+}$ embryos developed an autopodial skeleton, which is indistinguishable from those of wild type littermates. (B, E, H) *Gli3*$^{\Delta 699/-}$ embryos were highly polydactylous and displayed an obvious A/P asymmetry with anterior biphalangeal digits and posterior triphalangeal digits. (C, F, I) Predominantly, forelimbs of *Gli3*$^{\Delta 699/\Delta 699}$ embryos were polydactylous, whereas hindlimbs developed five digits. Both fore- and hindlimbs developed an increased share of biphalangeal digits. Please note that anterior digits appear correctly specified since they display an anatomy comparable to their wild type counterparts. However, posterior digits show various severe malformations such as fusions of metapodial elements and incorrect segmentation of phalanges.

apparent in the general shortness of the digits and the increased share of biphalangeal digits (Figs. 2F, I). At the same time, posterior digit identities are severly compromised. The disturbance of posterior morphogenesis manifests in various degrees of fusions between the cartilage elements of the metapodium and the digits (Figs. 2F, I). The anteriorization of the limb buds of *Gli3*$^{\Delta 699/\Delta 699}$ is a clear sign of increased GLI3 repressor activity during anteroposterior patterning of the mutant limb bud (Hill et al., 2007). As yet, however, it was unclear, whether the malformation of posterior digits was merely a dosage effect or whether indeed essential functions of GLI3-FL were missing in those mutant mice. In other words, it remained to be ascertained whether GLI3 repressor activity is sufficient to specify the full range of anteroposterior digit identities.

Here, we used the combination of a *Gli3*$^{\Delta 699}$ and a *Gli3*$^{-}$ allele to decrease GLI3$^{\Delta 699}$ levels while still retaining a GLI3-FL-free situation. *Gli3*$^{\Delta 699/-}$ embryos showed an increase in polydactyly when compared to *Gli3*$^{+/-}$ (Figs. 2B, E, H; compare to Figs. 1D, I, N). That result is in line with the previously reported finding that GLI3$^{\Delta 699}$ is less potent than wild type GLI3 in restraining digit numbers (Hill et al., 2007). In fact, the average extent of polydactyly of *Gli3*$^{\Delta 699/-}$ embryos was even close to that of *Gli3*$^{-/-}$ (Table 1). However, in stark contrast to the situation in *Gli3*$^{-/-}$ embryos, all autopods of *Gli3*$^{\Delta 699/-}$ embryos had a very clear anteroposterior asymmetry, which was also confirmed by bone and cartilage stainings. Being biphalangeal and shorter than their more posterior counterparts, the most preaxial digits of *Gli3*$^{\Delta 699/-}$ embryos always displayed the full set of anterior digit identity (Figs. 2E, H). Furthermore, it is important to stress, that the posterior triphalangeal digits were also well-formed and indistinguishable from posterior digits in wild type littermates. The well patterned autopodial skeleton of *Gli3*$^{\Delta 699/-}$ embryos thus reveals that the posterior malformations of homozygous *Gli3*$^{\Delta 699/\Delta 699}$ embryos are indeed caused by the dosage effect of increased GLI3 repressor activity

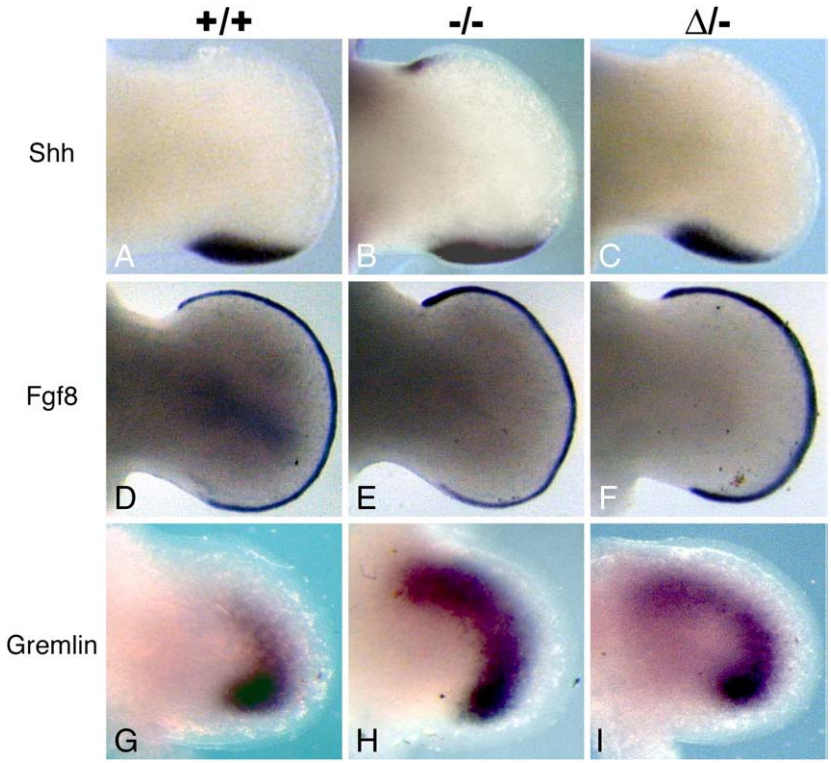

Fig. 3. Markers of the SHH/FGF feedback loop. Expression of *Shh* (A–C) in hindlimb buds, *Fgf8* (D–F) and *Gremlin* (G–I) in forelimb buds at E10.5 (G–I) and E11.5. (A–F) Anterior up-regulation of *Shh* in *Gli3*$^{-/-}$. *Shh* expression in *Gli3*$^{\Delta 699-}$ was normal. (D–F) *Gli3*$^{-/-}$ showed increased anterior expansion of *Fgf8* expression. In *Gli3*$^{\Delta 699/-}$, *Fgf8* expression was not anteriorly expanded, however, anterior *Fgf8* expression appeared more intense than in wild type littermates. (G–I) *Gremlin* expression was anteriorly expanded in *Gli3*$^{-/-}$ limb buds. A similar expansion of the *Gremlin* expression domain was observed in *Gli3*$^{\Delta 699/-}$, albeit at a much lower expression level.

rather than by a lack of essential GLI3-FL functions. Consequently, we propose that full-length GLI3 is dispensable for the formation of normal anterior and posterior digit identities. Nevertheless, we cannot exclude that GLI3-FL contributes to other parameters of limb development, such as the regulation of digit number, for example.

ZPA and AER activity in Gli3$^{\Delta 699/-}$ limb buds

There are two main signaling centers in the early limb bud, which are the apical ectodermal ridge (AER) and the zone of polarizing activity (ZPA). The ZPA is a posteriorly located group of mesodermal cells, which are characterized by *Shh* expression (Fig. 3A; Riddle et al., 1993). Similar to many other polydactylous mouse mutants, *Gli3*$^{-/-}$ embryos display ectopic anterior *Shh* expression, which is most prominent in the hindlimb bud (Fig. 3B). However, despite the similarly pronounced polydactyly of *Gli3*$^{\Delta 699/-}$ embryos, there was no anterior *Shh* expression and the posterior expression domain was normal in both fore- and hindlimbs (Fig. 3C).

The AER promotes the outgrowth of the limb bud by releasing FGF factors, which keep the underlying mesenchyme in a proliferative state (Boulet et al., 2004). Genetic analysis has shown that *Fgf8* mediates the most important activities of the AER (Lewandoski et al., 2000; Sun et al., 2002). *Fgf8* is expressed in the entire AER, which runs along the distal anteroposterior axis of the limb bud (Fig. 3D). The thickness of the AER and hence the *Fgf8* expression is decreased in the anterior-most part of the limb bud at this developmental stage (Fig. 3D). In *Gli3*$^{-/-}$ embryos, *Fgf8* expression was expanded anteriorly up to the presumptive border of zeugo- and autopod, i.e. the wrist region (Fig. 3E). In addition, there was no reduction in the thickness of the anterior part of the AER visible at that stage. Expression analysis of the limbs of *Gli3*$^{\Delta 699/-}$ embryos revealed no expansion of the AER (Fig. 3F). However, in contrast to the wild type situation, the AER did not thin out as much in the anterior part (Fig. 3F).

The reciprocal positive interaction of the two main signaling centers, AER and ZPA, has been termed the SHH/FGF feedback loop and it is pivotal in regulating limb bud outgrowth and digit number (reviewed in Talamillo et al., 2005). *Gremlin*, which is expressed in the posterior distal mesenchyme of the limb bud (Fig. 3G), is a key player in the maintenance of the SHH/FGF feedback loop (Khokha et al., 2003). In *Gli3*$^{-/-}$ limb buds, *Gremlin* expression is anteriorly expanded (Fig. 3H). The expression domain of *Gremlin* in *Gli3*$^{\Delta 699/-}$ limb buds was also anteriorly expanded, albeit at a reduced level of expression (Fig. 3I).

The increased integrity of the anterior AER and the mild up-regulation of *Gremlin* expression in *Gli3*$^{\Delta 699/-}$ limb buds are in line with the pronounced polydactyly observed in older *Gli3*$^{\Delta 699/-}$ embryos. Since the AER contributes to the control of the number of phalanges in developing digits (Sanz-Ezquerro and Tickle, 2003), it is

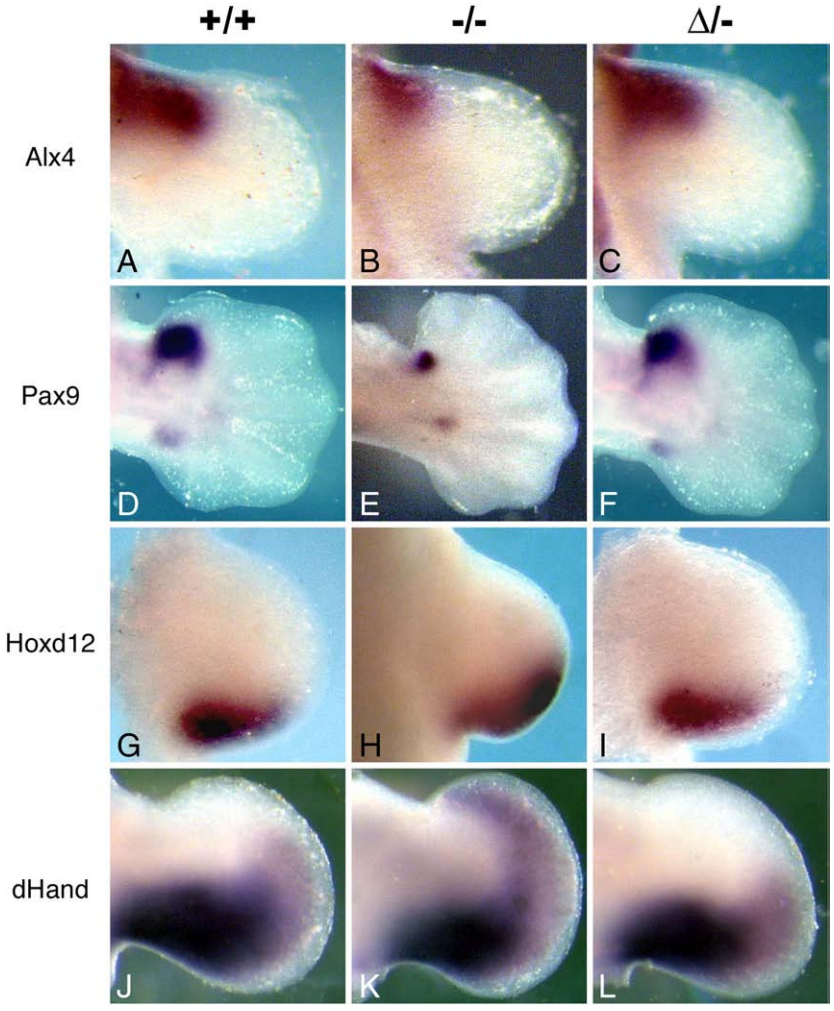

Fig. 4. Marker gene expression of the anteroposterior polarity. Whole-mount in situ hybridizations of forelimb buds showing gene expression involved in A/P patterning. (A–C) In *Gli3*$^{-/-}$, *Alx4* expression was considerably reduced whereas it was normal in *Gli3*$^{\Delta 699/-}$. (D–F) Anterior *Pax9* expression was drastically reduced in *Gli3*$^{-/-}$ but showed normal intensity in *Gli3*$^{\Delta 699/-}$. (G–I) Posterior restriction of *Hoxd12* was weakened upon loss of *Gli3* but was normal in *Gli3*$^{\Delta 699/-}$. (J–L) *dHand* expression was anteriorly expanded in *Gli3*$^{-/-}$ limb buds. Generally, *dHand* expression was normal in *Gli3*$^{\Delta 699/-}$ embryos. In some cases, however, posterior restriction of *dHand* expression was mildly increased compared to wild type littermates.

important to stress that the increased number of preaxial biphalangeal digits in *Gli3*$^{\Delta 699/-}$ embryos cannot be ascribed to a premature disintegration of the anterior AER in those hemizygous mutants.

Analysis of anteroposterior specific gene expression

Despite lacking the full-length GLI3 isoform, *Gli3*$^{\Delta 699/-}$ mutants produce limbs, which appear to be properly patterned along the anteroposterior axis. To check whether this appearance is truly based on the establishment of a normal A/P patterning, we analyzed molecular markers of anteroposterior patterning.

The transcription factor ALX4 is expressed in the anterior mesenchyme of the early limb bud (Fig. 4A). *Alx4*$^{-/-}$ mutants display ectopic anterior ZPA formation and inappropriate A/P patterning (Qu et al., 1997). Anterior *Alx4* expression depends on GLI3 function since *Alx4* expression is markedly reduced in Gli3$^{-/-}$ (Fig. 4B). However, *Alx4* expression is normal in *Gli3*$^{\Delta 699/-}$ embryos (Fig. 4C). PAX9 has been reported to act downstream of GLI3 in autopodial development and to contribute to the pattern formation of the anterior skeletogenic mesenchyme (Peters et al., 1998; McGlinn et al., 2005). Targeted loss of PAX9 results in preaxial digit duplication (Peters et al., 1998). *Pax9* expression in the murine limb is first observed at E11.5 (Neubüser et al.,

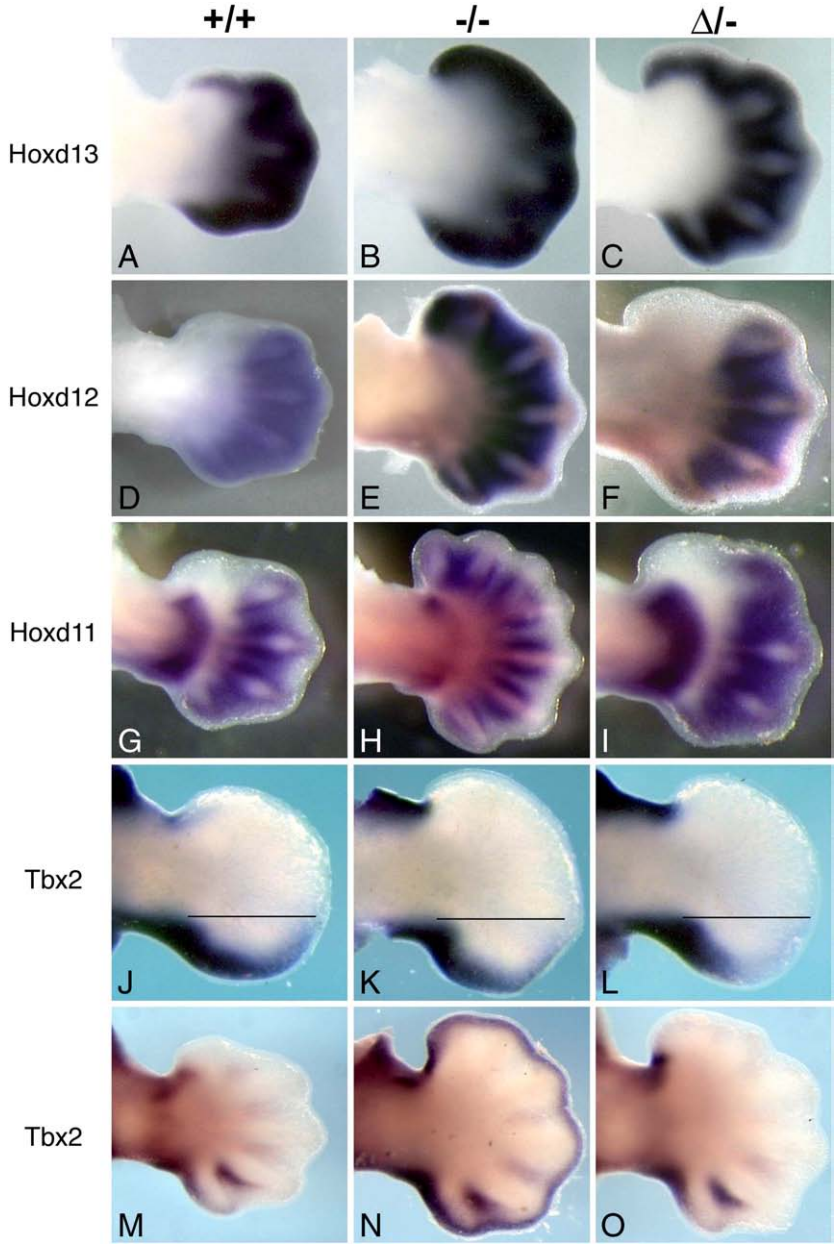

Fig. 5. Molecular digit identity. Whole-mount in situ hybridizations showing expression of marker genes connected to digit identity at E12.5 (A–I; M–O), and E11.5 (J–L) in forelimb buds. (A–C) All digit condensations of the three assessed genotypes showed *Hoxd13* expression. (D–F) *Hoxd12* expression was expanded into the anterior-most digit condensation in *Gli3*$^{-/-}$. In contrast, in *Gli3*$^{\Delta 699/-}$ the anterior region, which was devoid of *Hoxd12* expression, was larger than in wild type. (G–I) Similar to *Hoxd13*, all digit condensations of *Gli3*$^{-/-}$ embryos showed *Hoxd11* expression. Expression of *Hoxd11* in its proximal domain is markedly weakened in *Gli3*$^{-/-}$ embryos. In *Gli3*$^{\Delta 699/-}$ embryos, anterior digit condensations are free of *Hoxd11* expression, at the same time, proximal *Hoxd11* expression is at the normal level. (J–L) At E11.5, the anterior expansion of the autopodial expression of *Tbx2* was rather normal in both *Gli3*$^{-/-}$ and *Gli3*$^{\Delta 699/-}$ limb buds (marked by black lines). However, the intensity of the distal staining was weaker in both *Gli3*$^{-/-}$ and *Gli3*$^{\Delta 699/-}$ limb buds than in wild type embryos. (M) At E12.5, *Tbx2* was expressed in a proximal anterior and a proximal posterior domain in the wild type. Furthermore, strong *Tbx2* expression was detected in the interdigital region between digit 5 and 4. A thin band of expression was also seen in the distal mesenchyme from digit 5 to 4. (N) In *Gli3*$^{-/-}$ embryos, that distal band of *Tbx2* expression spannend the full anteroposterior axis. Expression in the posterior-most interdigital region seemed unaffected by the loss of GLI3. (O) The expression pattern of *Tbx2* in *Gli3*$^{\Delta 699/-}$ was essentially as in the wild type, except for a slight expansion of the distal expression domain, which in somes cases was extended up to the central digits.

1995). We investigated *Pax9* as a late anterior marker at E12.5. In wild type embryos, *Pax9* was expressed in a very prominent anterior domain and in a much weaker posterior domain (Fig. 4D). In $Gli3^{-/-}$ limb buds, posterior *Pax9* expression persisted, whereas the anterior domain was strongly downregulated (Fig. 4E). In contrast, in $Gli3^{\Delta 699/-}$ limb buds the pattern of *Pax9* expression was normal comprising a strong anterior expression and a weak posterior expression domain (Fig. 4F).

Recent reports emphasized a role of HOXD proteins in both early and late patterning events in the embryonic limb bud (Zakany et al., 2004). At E10.5, early *Hoxd12* expression is restricted to the posterior proximal mesenchyme (Fig. 4G). When GLI3 function was missing, *Hoxd12* expression extended anteriorly in the distal mesenchyme (Fig. 4H). $Gli3^{\Delta 699/-}$ limb buds showed an intact posterior restriction of *Hoxd12* expression (Fig. 4I). Next, we looked for expression of *dHand*, which is expressed in posterior and distal limb bud mesenchyme at E11.5 (Fig. 4J). *dHand* expression is up-regulated under the influence of SHH signaling (Charité et al., 2000; Fernandez-Teran et al., 2000) and is repressed in the anterior limb bud by GLI3 (te Welscher et al., 2002a). In $Gli3^{-/-}$ limbs, *dHand* expression was expanded anteriorly (Fig. 4K). In $Gli3^{\Delta 699/-}$ limbs, distal expression of *dHand* was slightly reduced in some cases but usually normal (Fig. 4L and data not shown). Thus, analysis of A/P markers clearly suggested an intact anteroposterior molecular patterning and thus confirmed the interpretation of limb morphology.

Analysis of molecular digit identity

The range of identified molecular markers of digit identity is anything but wide. That is probably due to the fact that all digits are constructed from the very same components. The most obvious anatomical difference exists between the biphalangeal anterior and the triphalangeal posterior identities. The expression pattern of *Hoxd* genes is exceptionally helpful in ascertaining the anterior-most digit identity on the molecular level. *Hoxd* genes are expressed in the forming autopod of mice and are thought to impart a dose-dependent mechanism for proliferation and growth of phalangeal structures (Zakany et al., 1997; Zakany and Duboule, 1999). At E12.5, *Hoxd13* is expressed in all digit condensations in the wild type (Fig. 5A). *Hoxd13* expression is also found in all digit condensations of the two mutant genotypes (Figs. 5B, C). However, in the wild type, digit 1 contrast with all other digits in that it displays absence of *Hoxd12* expression (Fig. 5D; Chiang et al., 2001). In $Gli3^{-/-}$ limb buds, on the other hand, *Hoxd12* was expressed equally strong in all digit condensations (Fig. 5E). In contrast, $Gli3^{\Delta 699/-}$ limbs showed continous *Hoxd12* expression only in four posterior digit condensations (Fig. 5F). The anterior region that was free of *Hoxd12* expression was considerably larger than in wild type embryos (compare Figs. 5F and D). To accommodate recent reports, which suggested different functions of the 5′ HOXD proteins we completed our analysis by assessing *Hoxd11* expression as well (Kmita et al., 2002). The distal autopodial pattern of *Hoxd11* expression was very similar to that of *Hoxd12* in all three genotypes. There was an anterior region free of *Hoxd11* expression both in wild type and $Gli3^{\Delta 699/-}$ limb buds, whereas all digit condensations of $Gli3^{-/-}$ embryos displayed *Hoxd11* expression (Figs. 5G–I). In contrast to *Hoxd12*, however, the expression pattern of *Hoxd11* comprises an additional proximal domain in the wrist region (Fig. 5G). In the $Gli3^{-/-}$ mutant, that proximal expression was very weak especially in the central part (Fig. 5H). That may, at least in part, be responsible for the disorganization of the GLI3 deficient wrist, since HOXD11 has been shown to be important for the correct formation of the carpals (Davis and Capecchi, 1994). In the $Gli3^{\Delta 699/-}$ mutant, however, the proximal domain of *Hoxd11* expression was of equal intensity as in the wild type (Fig. 5I).

In contrast to $Gli3^{\Delta 699/-}$ mutants, homozygous $Gli3^{\Delta 699/\Delta 699}$ mutants develop malformations of the posterior digits (Figs. 2E, H compare to F, I). The considerable repression of *Tbx2* in $Gli3^{\Delta 699/\Delta 699}$ mutants had been suggested to play a role in these posterior malformations since evidence exists that TBX2 is necessary for the proper formation of the digits 4 and 5 (Hill et al., 2007; Suzuki et al., 2004). At E11.5, the posterior autopodial expression of *Tbx2* was similar in all three genotypes (Figs. 5J–L). Nevertheless, *Tbx2* expression was weaker in the distal mesenchyme of both $Gli3^{-/-}$ and $Gli3^{\Delta 699/-}$ mutants than in wild type embryos (Figs. 5J–L). However, the reduction in *Tbx2* expression in $Gli3^{\Delta 699/-}$ mutants was much less pronounced than in $Gli3^{\Delta 699/\Delta 699}$ mutants (Hill et al., 2007). In fact, in all three genotypes shown here the most distal tip of *Tbx2* expression was at one horizontal level with the proximal *Tbx2* expression domain around the presumptive wrist region (marked by black lines in Figs. 5J–L). At E12.5, *Tbx2* was expressed strongest at the anterior and posterior margin of the autopod and in the interdigital region between digit 4 and 5 (Fig. 5M). There was also expression of *Tbx2* in the mesenchyme at the tip of digit 5 and, very weakly, digit 4 (Fig. 5M). $Gli3^{-/-}$ mutants also showed strong expression in the interdigital region between digit 4 and 5 (Fig. 5N). Apart from that, however, they displayed a very remarkable change in the pattern of *Tbx2* expression. The expression domain in the distal mesenchyme extended fully along the anteroposterior axis of the limb bud such that

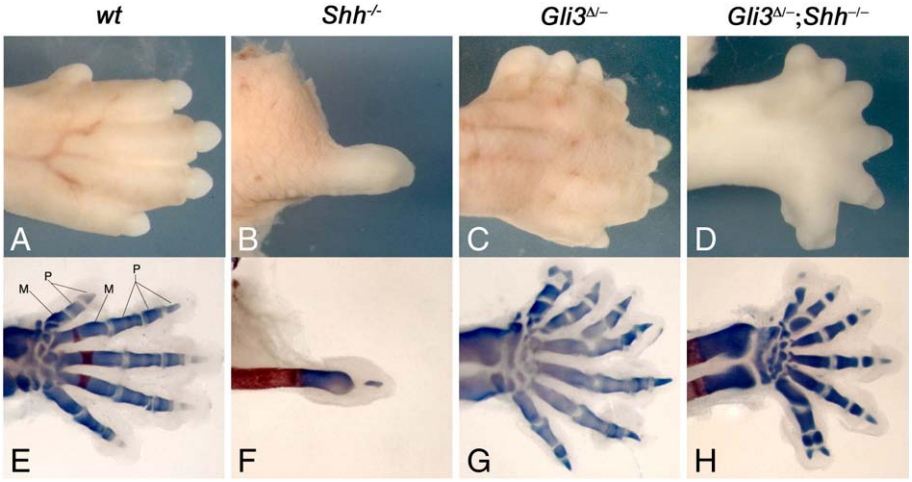

Fig. 6. Skeletal anatomy in the presence and in the absence of SHH at E14.5. Dorsal view of untreated (A–D) and Alcian Blue/Alizarin Red stained fore paws (E–H) at E16.5. Anterior is upwards and distal is towards the right. M: metacarpal; P: phalanges. (A, E) The digits are clearly recognizable in the wild type. (B, F) Forelimbs of $Shh^{-/-}$ embryos carry merely rudiments of digits. (C, G) The limbs of $Gli3^{\Delta 699/-}$ display polydactyly and anterior as well as posterior digit identities. (D, H) Despite the loss of SHH, the limbs of $Shh^{-/-}$;$Gli3^{\Delta 699/-}$ mutants did also produce 7–8 digit primordia with an obvious A/P asymmetry.

the anterior and posterior expression domains were connected by a thin line of *Tbx2* expression (Fig. 5O). In stark contrast, *Tbx2* expression in *Gli3*$^{\Delta 699/-}$ mutants was essentially as in the wild type, except for an additional faint expression of *Tbx2* at the distal tip of the central digit ('3') in some specimen (Fig. 5O and data not shown).

Hence, the molecular analysis of both anterior and posterior digit identity markers revealed striking congruence between the expression pattern of *Gli3*$^{\Delta 699/-}$ and wild type limb buds. Appreciable divergence between wild type and *Gli3*$^{\Delta 699/-}$ mutant expression patterns existed only in the anterior region, where the increased repression of *Hoxd11/12* in *Gli3*$^{\Delta 699/-}$ limb buds reflected the additional digit 1 identities in the mutant.

Digit development of Gli3$^{\Delta 699/-}$ *mutants in the absence of SHH*

The recent analyses of the *Shh*$^{-/-}$;*Gli3*$^{-/-}$ double mutant suggested that the nearly digitless *Shh*$^{-/-}$ phenotype was the result of excessive GLI3 processing (Litingtung et al., 2002; te Welscher et al., 2002a,b). Furthermore, the indistinguishability of *Shh*$^{-/-}$;*Gli3*$^{-/-}$ and *Gli3*$^{-/-}$ single mutants implied that every impact of SHH on limb development is dependent on the presence of processable GLI3. In the case of the *Gli3*$^{\Delta 699/-}$ mutant SHH is definitely unable to interfere with GLI3 function on the level of posttranslational processing because of the lack of GLI3-FL. Our above presented analyses have revealed considerable evidence that A/P patterning in the limbs of *Gli3*$^{\Delta 699/-}$ mutants is remarkably normal. Therefore, we were interested to see whether the removal of SHH would entail any effect on the identity and number of digits in that particular background.

The first remarkable consequence was the early death of the double mutant *Shh*$^{-/-}$;*Gli3*$^{\Delta 699/-}$ embryos, which mostly died around E14.5 even though the respective single mutants survive much longer. Nevertheless, we were able to collect several E16.5 specimen to allow for bone and cartilage staining of the digits (Figs. 6A, E). As reported, the forelimbs of *Shh*$^{-/-}$ embryos carry merely rudiments of digits (Figs. 6B, F; Chiang et al., 2001). The limbs of *Gli3*$^{\Delta 699/-}$ embryos maintained the familiar phenotype also in the interbred background, displaying polydactyly and anterior as well as posterior digit identities (Figs. 6C, D; compare to Figs. 2C, G). Remarkably, despite the loss of SHH, the limbs of *Shh*$^{-/-}$;*Gli3*$^{\Delta 699/-}$ mutants did also produce 7–8 digit primordia (Figs. 6D, H). Furthermore, those limbs still displayed an obvious A/P asymmetry. The overall pattern of cartilage condensations is similar to that of *Gli3*$^{\Delta 699/-}$ and seems thus largely unaffected by the loss of SHH (compare Figs. 6G and H). Nevertheless, there are some differences in the shape of the limb buds of *Gli3*$^{\Delta 699/-}$ and *Shh*$^{-/-}$;*Gli3*$^{\Delta 699/-}$ littermates. In wild type and in *Gli3*$^{\Delta 699/-}$ embryos digit length reaches its climax in the centrally positioned digit, whereas in *Shh*$^{-/-}$;*Gli3*$^{\Delta 699/-}$ littermates digit length seemed to increase more steadily and the increase persisted along the entire anteroposterior axis up to the most posterior digit (compare Figs. 6A, C and D).

However, despite those differences in details between the limbs of *Gli3*$^{\Delta 699/-}$ embryos and *Shh*$^{-/-}$;*Gli3*$^{\Delta 699/-}$ littermates it must be noted that *Shh*$^{-/-}$;*Gli3*$^{\Delta 699/-}$ retain an obvious anteroposterior asymmetry even in the absence of SHH. Consequently, SHH does not contribute substantially to the remarkable A/P asymmetry of *Gli3*$^{\Delta 699/-}$ embryos.

Several studies have indicated that transcriptional regulation of *Gli3* is dependent on SHH activity (Schweitzer et al., 2000; Marigo et al., 1996). To investigate this effect in the context of the *Gli3*$^{\Delta 699}$ mutant we analyzed *Gli3* regulation in limb buds. In the wild type, *Gli3* is expressed in an anteroposterior asymmetric fashion (Fig. 7A). The absence of SHH indeed resulted in a complete loss of anteroposterior asymmetry of *Gli3* expression (Fig. 7B), However, to that extent this was only observed when wild type i.e. processable GLI3 was present since the *Gli3* expression pattern in *Gli3*$^{-/-}$ mutants retained a clear (even though weakenend) A/P asymmetry (compare Figs. 7B and D, F). The *Gli3* expression pattern in the *Gli3*$^{\Delta 699/-}$ mutant was even indistinguishable from that of a wild type specimen (compare Figs. 7A and G) and it remained unaffected even when SHH was absent (Fig. 7H). Thus, although normally both SHH and GLI3 contribute to the regulation of the *Gli3* expression pattern, neither of the two is imperative for the fundamental anteroposterior asymmetry of *Gli3* expression. The observation of an anteroposterior gradient of *Gli3*$^{\Delta 699}$ expression explains how the formation of both anterior and posterior digits is accomplished in the limb buds of *Gli3*$^{\Delta 699}$ mutants despite SHH being unable to influence the anteroposterior grading of GLI3 repressor function by inhibiting postranslational processing.

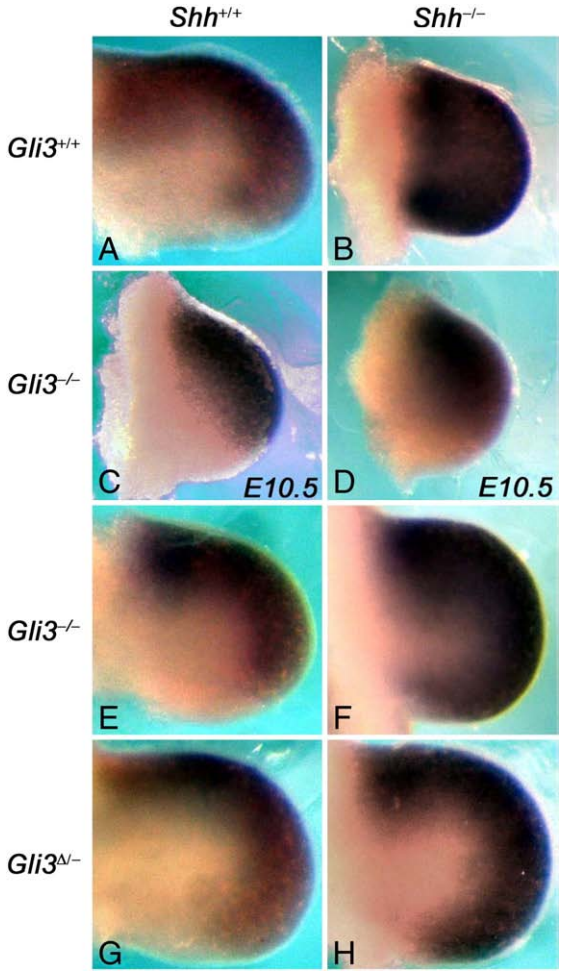

Fig. 7. *Gli3* expression pattern in *Shh* and *Gli3* mutants. Whole-mount in situ hybridizations showing *Gli3* expression at E10.5 (C, D) and E11.5 in forelimb buds. (A) In the wild type, *Gli3* is expressed with an obvious anteroposterior asymmetry with the lowest expression in the posterior part of the limb bud. (B) In the Shh$^{-/-}$ mutant, which is characterized by excessive levels of GLI3R, *Gli3* was expressed throughout the whole limb bud at a high level. (C, E) Normal anterior prevalence of *Gli3* expression was obvious in *Gli3*$^{-/-}$ mutants, both at E10.5 and E11.5. (D) At E10.5, the *Gli3* expression pattern was unaffected by the combined loss of both GLI3 and SHH. (F) At E10.5, *Gli3* expression tended to be slightly posteriorly expanded but a solid anterior prevalence of *Gli3* expression still persisted. (G, H) The *Gli3* expression pattern in the *Gli3*$^{\Delta 699/-}$ mutant was normal and remained unaffected even when SHH was absent. Thus, an anteroposterior gradient of GLI3$^{\Delta 699}$ is established in these mutants to account for the formation of both anterior and posterior digits.

Discussion

Quantitative and qualitative effects of GLI3/GLI3$^{\Delta 699}$ *on autopod development*

The importance of GLI3 in the context of limb development has been very clear since mutations in *Gli3* have been identified as the

genetic cause of the extra-toes mutation (*Gli3*$^{-}$) in mice and multiple congenital diseases in man, all of which are associated with limb malformations (Hui and Joyner, 1993; Biesecker, 1997; Büscher et al., 1998, Nieuwenhuis and Hui, 2005). Many publications have since stressed the contribution of GLI3 to various aspects of vertebrate limb development such as the regulation of limb bud size, digit identities and the timing of chondrogenesis (Litingtung et al., 2002; te Welscher et al., 2002b; Ahn and Joyner, 2004; McGlinn et al., 2005). In addition, it had always been quite obvious that there was a quantitative component in the function of GLI3 because the phenotype of homozygous mice is much more pronounced than that of heterozygous animals. Still as yet no one has ever assessed how gradual changes in the quantity of GLI3 affect limb development. That is surprising in consideration of the *Gli3* related human diseases, which display limb defects that are often distinct and characteristic for individual diseases. A detailed assessment of the effect of quantitative changes in GLI3 levels might help in understanding the basis of the human spectrum of symptoms. So here for the first time we compared how the different defects, which are apparent in *Gli3*$^{-/-}$ embryos, are sequentially restored upon a gradual rise in GLI3 levels.

Previous reports emphasized the negative effect of GLI3 on the number of digits (Litingtung et al., 2002; te Welscher et al.; 2002b). While confirming these reports, our results implied a so far unreported threshold-like mechanism in the regulation of digit numbers by GLI3. The degree of polydactyly does not decrease from *Gli3*$^{-/-}$ via *Gli3*$^{Pdn/-}$ to *Gli3*$^{Pdn/Pdn}$ embryos. A steep decline of polydactyly is only seen in the step from *Gli3*$^{Pdn/Pdn}$ to *Gli3*$^{+/-}$ embryos. In this regard, it is also interesting to note that regulation of digit number in fore- and hindlimbs seems to be differentially susceptible to a reduction of GLI3 levels. In general, the forelimb exhibits a more pronounced polydactyly than the hindlimb (Table 1). It remained unclear, what causes this divergence, since we did not find any fore or hindlimb specific changes in expression patterns. In this respect, it is important to bear in mind that even in the wild type, there is still a very limited understanding of how a largely mutual patterning program ultimately results in the obvious anatomical deviations of anterior vs. posterior extremities (reviewed in Logan, 2003).

Besides causing polydactyly, the complete loss of GLI3 function is accompanied by a defective formation of the proximal phalanges. In fact, the segmentation of proximal phalanges is the decisive step in translating molecular patterning into digital identity, because the formation of the distal phalanx is independent of those processes, which determine the number of phalanges, i.e. digit identity (Sanz-Ezquerro and Tickle, 2003). We could demonstrate that a small amount of GLI3 protein in *Gli3*$^{Pdn/-}$ embryos is already sufficient to facilitate phalanx morphogenesis. Concomitantly, it became obvious that normal A/P asymmetry is not established at this low GLI3 level because even anteriorly located digits displayed an anatomy typical of posterior digit identities. However, in contrast to digit number, A/P asymmetry improved steadily with increasing GLI3 levels. A certain recovery of A/P asymmetry was seen in *Gli3*$^{Pdn/Pdn}$, whereas it was not until heterozygous *Gli3*$^{+/-}$ embryos that anteroposterior polarity was fully established (as defined by the presence of unequivocal anterior and posterior digit identities in 100% of assessed embryos).

In a previous report, we could demonstrate that GLI3$^{\Delta 699}$ fulfills the role that has been proposed for GLI3R in the specification of digit identities (Hill et al., 2007). Therefore, *Gli3*$^{\Delta 699}$ mutants allow for the specific assessment of GLI3R function in that particular context. Homozygous *Gli3*$^{\Delta 699/\Delta 699}$ mutants develop anterior digit identities but display malformations of posterior digits (Hill et al., 2007). As yet, it remained unclear whether these posterior distortions were the consequence of an excess of GLI3 repressor function or whether they provided an indication of an essential GLI3-FL function that was missing in *Gli3*$^{\Delta 699/\Delta 699}$ mutants. Two preceding reports have argued particularly for a requirement of both GLI3 isoforms (Litingtung et al., 2002; Wang et al., 2007). Litingtung et al. suggested that the balance of GLI3-FL:GLI3R instead of absolute GLI3R levels would specify the different digit identities (Litingtung et al., 2002). That hypothesis was supported by a recent publication (Wang et al., 2007). In the setting by Wang et al., *Gli3* was genetically modified so that four PKA-sites, which are required for GLI3 processing, were destroyed in the resulting protein, which was termed GLI3^{P1-4}. Thus, GLI3^{P1-4} was rendered unprocessable and was interpreted as an equivalent substitute for GLI3-FL. Wang et al. have reported that GLI3^{P1-4} produced correct anteroposterior digit identities only in combination with GLI3$^{\Delta 699}$ in *Gli3*$^{\Delta 699/P1-4}$ mutants (Wang et al., 2007). That observation led to the interpretation of an essential requirement for both GLI3 isoforms in the anteroposterior patterning of the limb bud (Wang et al., 2007). Contrary to these reports, we showed here that the expression patterns of anteroposterior markers in the limb buds of *Gli3*$^{\Delta 699/-}$ mutants displayed no significant alterations when compared to wild type embryos. Furthermore, at later developmental stages *Gli3*$^{\Delta 699/-}$ embryos formed correctly specified anterior as well as posterior digit identities in the complete absence of the GLI3-FL isoform. Concomitantly, it became evident that the commonly observed posterior malformations of *Gli3*$^{\Delta 699/\Delta 699}$ embryos are not the result of a lack of GLI3-FL. Instead, lowering the level of GLI3$^{\Delta 699}$, as in *Gli3*$^{\Delta 699/-}$ embryos, is sufficient to prevent those posterior malformations.

These results clearly contrast with the above quoted report, which argues for an essential contribution of both GLI3 isoforms (Wang et al., 2007). However, the limb phenotype of combined *Gli3*$^{\Delta 699/P1-4}$ mutants is in fact indistinguishable from that of *Gli3*$^{\Delta 699/-}$ mutants. Thus, no additional gain of 'A/P normality' could be provoked by the presence of the GLI3-FL representative GLI3^{P1-4}. Consequently, we propose that the contribution of the GLI3-FL isoform is negligible if at all existent in the specification of digit identities. We suggest, that proper A/P patterning is achieved solely by GLI3 repressor activity with no active contribution by GLI3-FL.

The impact of a primal prototype patterning

The fact that *Gli3*$^{\Delta 699/-}$ embryos develop anterior as well as posterior digit identities argues strongly in favor of a sole necessity for the GLI3 repressor isoform in A/P patterning. However, looking at this from a different angle eventually raises the question of how different digit identities can at all be specified when the SHH-dependent regulation of GLI3 processing is omitted in *Gli3*$^{\Delta 699/-}$ mutants. After all, the current concept of A/P patterning holds that increments of GLI3 activity have to be established from the anterior to the posterior margin of the limb bud. At present, that A/P grading of GLI3 activity is believed to be achieved by the SHH-controlled, inhomogeneous conversion rate of GLI3-FL to GLI3R. Due to its already truncated nature, however, GLI3$^{\Delta 699}$ is resistant to such posttranslational regulation of processing by SHH. Therefore our results clearly argue for the existence of an additional mechanism that ensures grading of GLI3 activity separate from GLI3 processing in *Gli3*$^{\Delta 699/-}$ mutants. One obvious candidate for such a mechanism would be the transcriptional regulation of *Gli3* since *Gli3* itself is expressed in an anteroposterior graded fashion with expression levels that decline from anterior to posterior (Büscher and Rüther, 1998; Fig. 7). According to previous reports, SHH might additionally possess the potential to regulate *Gli3* on the transcriptional level and thus independent of its processability (Schweitzer et al., 2000; Marigo et al., 1996). By comparing two systems devoid of processable GLI3, namely *Gli3*$^{\Delta 699/-}$ and *Gli3*$^{\Delta 699/-}$;*Shh*$^{-/-}$ mutants, we indeed found some differences between the two resulting phenotypes. That remarkable fact illustrates that the action of SHH indeed reaches beyond merely restricting the conversion rate of GLI3-FL. However, the removal of SHH entailed only relatively minor effects and did not affect the general A/P asymmetry in *Gli3*$^{\Delta 699/-}$;*Shh*$^{-/-}$ mutants. Conclusively, the establishment of the remarkably normal A/P asymmetry in *Gli3*$^{\Delta 699/-}$ mutants cannot be attributed to the action

of SHH. In concordance with this observation we found a normal *Gli3* expression pattern both in $Gli3^{\Delta 699/-}$ and in $Gli3^{\Delta 699/-}$;$Shh^{-/-}$ mutants (Fig. 7). Inevitably, one must wonder how the necessary anteroposterior grading of GLI3 repressor activity is achieved otherwise in $Gli3^{\Delta 699/-}$ mutants. Based on existing data it is possible to speculate on this and we suggest that the $Gli3^{-/-}$ mutant may give valuable insight into this matter.

In the literature, the digits of $Gli3^{-/-}$ mutants are commonly described as lacking any identity. However, detailed examination of bone and cartilage stainings reveals that the formation of the proximal phalanges tends to gradually improve towards the posterior side. In fact, the posterior-most digit of $Gli3^{-/-}$ limbs usually develops three phalanges, i.e. the basic anatomical criteria for classification of posterior digit identity. Admittedly, posterior digit identity is not fully established in the absence of GLI3, once again stressing the importance of GLI3 for patterning the full measure of the distal A/P axis. However, the skeletal remnant of A/P identity is also supported by the analysis of gene expression patterns. The expression of anterior markers (*Alx4*, *Pax9*) is greatly weakened but has not completely vanished in $Gli3^{-/-}$ limbs, whereas the expression pattern of posterior markers (*dHand*, *Tbx2*) may be anteriorly expanded but is by no means symmetrical (Figs. 4 and 5). It is thus noteworthy that a basic molecular A/P asymmetry is perpetuated even in the absence of GLI3. Furthermore, given the complete identicalness of $Gli3^{-/-}$ and $Gli3^{-/-}$;$Shh^{-/-}$ limb buds (Litingtung et al., 2002; te Welscher et al., 2002b) that basic molecular asymmetry must also be regarded as being independent of SHH. In fact, the expression pattern of *Gli3* itself is subject to this SHH/GLI3-independent prepattern as may be seen in the limb buds of $Gli3^{-/-}$;$Shh^{-/-}$ mutants, in which a solid anterior prevalence of *Gli3* expression persists that is very similar to the wild type pattern (Fig. 7).

In order to avoid confusion with the already assigned term 'prepattern', which denotes the interaction of GLI3 and DHAND in the early limb bud (te Welscher et al., 2002a), the herein described SHH/GLI3-independent basic asymmetry will be referred to as 'prototype pattern' in the following. The prevailing A/P asymmetry of *Gli3* expression in $Gli3^{-/-}$(;$Shh^{-/-}$) limb buds indicates that the early prototype pattern lays a scaffold, upon which the later higher order of A/P asymmetry that involves the action of GLI3 and SHH is grounded. Normally, at later developmental stages any sign of the earlier sketchy A/P patterning would be obscured by the reciprocal interaction of SHH and GLI3. Thus, the prototype pattern remains visible only in those cases where SHH is ineffective (i.e. *Shh* null mutation, unprocessable or missing GLI3) and where any efficacy of GLI3R is absent or too low to abrogate the basic SHH/GLI3-independent asymmetry. One of such cases is the $Gli3^{-/-}$ mutant. There, the prototype patterning is recognizable in the observed rudimentary morphological and molecular A/P asymmetry described above. Still, the considerably normal expression pattern of *Gli3* is of mere academic interest in those mutants since no higher order of asymmetry can be achieved because of the total lack of GLI3 function. In contrast to the situation in $Gli3^{-/-}$ mutants, however, $Gli3^{\Delta 699/-}$ embryos possess functional GLI3 repressor activity. Additionally, in the hemizygous $Gli3^{\Delta 699/-}$ embryos GLI3R activity is obviously sufficiently reduced in quantity to prevent the complete anteriorization of the limb bud and thus the strong ectopic *Gli3* expression throughout the limb bud that is observed in $Gli3^{+/+}$;$Shh^{-/-}$ embryos (Figs. 7, compare B with G and H). Therefore, an asymmetric *Gli3* expression pattern that is analogous to the anteroposterior gradient in the wild type is established in $Gli3^{\Delta 699/-}$ embryos (Fig. 7).

In summary, the rudiments of A/P asymmetry in the indistinguishable $Gli3^{-/-}$ and $Gli3^{-/-}$;$Shh^{-/-}$ embryos uncover a basic anteroposterior asymmetry that is independent of both GLI3 and SHH. The prevailing asymmetry of *Gli3* expression in $Gli3^{-/-}$(;$Shh^{-/-}$) and $Gli3^{\Delta 699/-}$(;$Shh^{-/-}$) embryos reveals that the *Gli3* expression pattern is itself subject to that primal patterning mechanism. Thus, the stunning formation of both anterior and posterior digit identities in $Gli3^{\Delta 699/-}$ embryos results from an anteroposterior gradient of GLI3 repressor function that is induced by a SHH/GLI3-independent prototype pattern.

Consequently, we propose to amend the current perception of how digits are specified. So far, the establishment of GLI3(R) increments along the A/P axis has been solely considered a consequence of posttranslational regulation by SHH signals. Here, we presented evidence that this mode of action is supported by a prototype pattern, which regulates *Gli3* independently from SHH. The control of the *Gli3* expression pattern is not the only conceivable but the most likely operational area of that SHH-independent basic regulative mechanism, which contributes to the GLI3-mediated A/P asymmetry in the embryonic limb bud.

Acknowledgments

We would like to thank Julia Fischer and Jürgen Knobloch for critically reading the manuscript. This work was supported by grants of the Deutsche Forschungsgemeinschaft and by the Düsseldorf Entrepreneurs Foundation.

References

Ahn, S., Joyner, A.L., 2004. Dynamic changes in the response of cells to positive hedgehog signaling during mouse limb patterning. Cell 118, 505–516.
Aza-Blanc, P., Kornberg, T.B., 1999. Ci: a complex transducer of the hedgehog signal. Trends Genet. 15, 458–462.
Aza-Blanc, P., Ramirez-Weber, F.A., Laget, M.P., Schwartz, C., Kornberg, T.B., 1997. Proteolysis that is inhibited by hedgehog targets Cubitus interruptus protein to the nucleus and converts it to a repressor. Cell 89, 1043–1053.
Bai, C.B., Auerbach, W., Lee, J.S., Stephen, D., Joyner, A.L., 2002. GLI2, but not GLI1, is required for initial SHH signaling and ectopic activation of the SHH pathway. Development 129, 4753–4761.
Biesecker, L.G., 1997. Strike three for GLI3. Nat. Genet. 17, 259–260.
Böse, J., Grotewold, L., Rüther, U., 2002. Pallister–Hall syndrome phenotype in mice mutant for GLI3. Hum. Mol. Genet. 11, 1129–1135.
Boulet, A.M., Moon, A.M., Arenkiel, B.R., Capecchi, M.R., 2004. The roles of Fgf4 and Fgf8 in limb bud initiation and outgrowth. Dev. Biol. 273, 361–372.
Büscher, D., Rüther, U., 1998. Expression profile of Gli family members and Shh in normal and mutant mouse limb development. Dev. Dyn. 211, 88–96.
Büscher, D., Grotewold, L., Rüther, U., 1998. The Xt allele generates a GLI3 fusion transcript. Mamm. Genome 9, 676–678.
Charité, J., McFadden, D.G., Olson, E.N., 2000. The bHLH transcription factor dHAND controls sonic hedgehog expression and establishment of the zone of polarizing activity during limb development. Development 127, 2461–2470.
Chiang, C., Litingtung, Y., Harris, M.P., Simandl, B.K., Li, Y., Beachy, P.A., Fallon, J.F., 2001. Manifestation of the limb prepattern: limb development in the absence of sonic hedgehog function. Dev. Biol. 236, 421–435.
Cohen Jr., M.M., 2003. The hedgehog signaling network. Am. J. Med. Genet. A 123A, 5–28.
Dai, P., Akimaru, H., Tanaka, Y., Maekawa, T., Nakafuku, M., Ishii, S., 1999. Sonic hedgehog-induced activation of the GLI1 promoter is mediated by GLI3. J. Biol. Chem. 274, 8143–8152.
Davis, A.P., Capecchi, M.R., 1994. Axial homeosis and appendicular skeleton defects in mice with a targeted disruption of hoxd-11. Development 120, 2187–2198.
Fernandez-Teran, M., Piedra, M.E., Kathiriya, I.S., Srivastava, D., Rodriguez-Rey, J.C., Ros, M.A., 2000. Role of dHAND in the anterior–posterior polarization of the limb bud: implications for the sonic hedgehog pathway. Development 127, 2133–2142.
Grotewold, L., Theil, T., Rüther, U., 1999. Expression pattern of Dkk-1 during mouse limb development. Mech. Dev. 89, 151–153.
Hill, P., Wang, B., Rüther, U., 2007. The molecular basis of Pallister–Hall associated polydactyly. Hum. Mol. Genet. 16, 2089–2096.
Hui, C.C., Joyner, A.L., 1993. A mouse model of greig cephalopolysyndactyly syndrome: the extra-toesJ mutation contains an intragenic deletion of the GLI3 gene. Nat. Genet. 3, 241–246.
Ingham, P.W., McMahon, A.P., 2001. Hedgehog signaling in animal development: paradigms and principles. Genes Dev. 15, 3059–3087.
Kasper, M., Regl, G., Frischauf, A.-M., Aberger, F., 2006. GLI transcription factors: mediators of oncogenic hedgehog signalling. EJC 42, 437–445.
Kang, S., Graham Jr., J.M., Olney, A.H., Biesecker, L.G., 1997. GLI3 frameshift mutations cause autosomal dominant Pallister–Hall syndrome. Nat. Genet. 15, 266–268.
Khokha, M.K., Hsu, D., Brunet, L.J., Dionne, M.S., Harland, R.M., 2003. Gremlin is the BMP antagonist required for maintenance of SHH and Fgf signals during limb patterning. Nat. Genet. 34, 303–307.
Kmita, M., Fraudeau, N., Herault, Y., Duboule, D., 2002. Serial deletions and duplications suggest a mechanism for the collinearity of Hoxd genes in limbs. Nature 420, 145–150.
Lewandoski, M., Sun, X., Martin, G.R., 2000. Fgf8 signalling from the AER is essential for normal limb development. Nat. Genet. 26, 460–463.

Litingtung, Y., Dahn, R.D., Li, Y., Fallon, J.F., Chiang, C., 2002. SHH and GLI3 are dispensable for limb skeleton formation but regulate digit number and identity. Nature 418, 979–983.
Logan, M., 2003. Finger or toe: the molecular basis of limb identity. Development 130, 6401–6410.
Marigo, V., Johnson, R.L., Vortkamp, A., Tabin, C.J., 1996. Sonic hedgehog differentially regulates expression of Gli and Gli3 during limb development. Dev. Biol. 180, 273–283.
McGlinn, E., van Bueren, K.L., Fiorenza, S., Mo, R., Poh, A.M., Forrest, A., Soares, M.B., Bonaldo Mde, F., Grimmond, S., Hui, C.C., Wainwright, B., Wicking, C., 2005. Pax9 and Jagged1 act downstream of GLI3 in vertebrate limb development. Mech. Dev. 122, 1218–1233.
Motoyama, J., Milenkovic, L., Iwama, M., Shikata, Y., Scott, M.P., Hui, C.C., 2003. Differential requirement for GLI2 and GLI3 in ventral neural cell fate specification. Dev. Biol. 259, 150–161.
Neubüser, A., Koseki, H., Balling, R., 1995. Characterization and developmental expression of Pax9, a paired-box-containing gene related to Pax1. Dev. Biol. 170, 701–716.
Nieuwenhuis, E., Hui, C.C., 2005. Hedgehog signaling and congenital malformations. Clin. Genet. 67, 193–208.
Ohlmeyer, J.T., Kalderon, D., 1998. Hedgehog stimulates maturation of Cubitus interruptus into a labile transcriptional activator. Nature 396, 749–753.
Park, H.L., Bai, C., Platt, K.A., Matise, M.P., Beeghly, A., Hui, C.C., Nakashima, M., Joyner, A.L., 2000. Mouse GLI1 mutants are viable but have defects in SHH signaling in combination with a GLI2 mutation. Development 127, 1593–1605.
Peters, H., Neubüser, A., Kratochwil, K., Balling, R., 1998. Pax9-deficient mice lack pharyngeal pouch derivatives and teeth and exhibit craniofacial and limb abnormalities. Genes Dev. 12, 2735–2747.
Qu, S., Niswender, K.D., Ji, Q., van der Meer, R., Keeney, D., Magnuson, M.A., Wisdom, R., 1997. Polydactyly and ectopic ZPA formation in Alx-4 mutant mice. Development 124, 3999–4008.
Riddle, R.D., Johnson, R.L., Laufer, E., Tabin, C., 1993. Sonic hedgehog mediates the polarizing activity of the ZPA. Cell 75, 1401–1416.
Sanz-Ezquerro, J.J., Tickle, C., 2003. Fgf signaling controls the number of phalanges and tip formation in developing digits. Curr. Biol. 13, 1830–1836.
Sasaki, H., Nishizaki, Y., Hui, C., Nakafuku, M., Kondoh, H., 1999. Regulation of GLI2 and GLI3 activities by an amino-terminal repression domain: implication of GLI2 and GLI3 as primary mediators of SHH signaling. Development 126, 3915–3924.
Schweitzer, R., Vogan, K.J., Tabin, C.J., 2000. Similar expression and regulation of Gli2 and Gli3 in the chicken limb bud. Mech. Dev. 98, 171–174.
Sun, X., Mariani, F.V., Martin, G.R., 2002. Functions of FGF signalling from the apical ectodermal ridge in limb development. Nature 418, 501–508.
Suzuki, T., Takeuchi, J., Koshiba-Takeuchi, K., Ogura, T., 2004. Tbx genes specify posterior digit identity through SHH and BMP signaling. Dev. Cell 6, 43–53.
Talamillo, A., Bastida, M.F., Fernandez-Teran, M., Ros, M.A., 2005. The developing limb and the control of the number of digits. Clin. Genet. 67, 143–153.
te Welscher, P., Fernandez-Teran, M., Ros, M.A., Zeller, R., 2002a. Mutual genetic antagonism involving GLI3 and dHAND prepatterns the vertebrate limb bud mesenchyme prior to SHH signaling. Genes Dev. 16, 421–426.
te Welscher, P., Zuniga, A., Kuijper, S., Drenth, T., Goedemans, H.J., Meijlink, F., Zeller, R., 2002b. Progression of vertebrate limb development through SHH-mediated counteraction of GLI3. Science 298, 827–830.
Thien, H., Rüther, U., 1999. The mouse mutation Pdn (*Polydactyly Nagoya*) is caused by the integration of a retrotransposon into the GLI3 gene. Mamm. Genome 10, 205–209.
Ueta, E., Maekawa, M., Morimoto, I., Nanba, E., Naruse, I., 2004. Sonic hedgehog expression in GLI3 depressed mouse embryo, Pdn/Pdn. Congenit. Anom. 44, 27–32.
Vortkamp, A., Gessler, M., Grzeschik, K.H., 1991. GLI3 zinc-finger gene interrupted by translocations in Greig syndrome families. Nature 352, 539–540.
Wang, Q.T., Holmgren, R.A., 1999. The subcellular localization and activity of *Drosophila cubitus interruptus* are regulated at multiple levels. Development 126, 5097–5106.
Wang, B., Fallon, J.F., Beachy, P.A., 2000. Hedgehog-regulated processing of GLI3 produces an anterior/posterior repressor gradient in the developing vertebrate limb. Cell 100, 423–434.
Wang, C., Rüther, U., Wang, B., 2007. The Shh-independent activator function of the full-length GLI3 protein and its role in vertebrate limb digit patterning. Dev. Biol. 305, 460–469.
Wild, A., Kalff-Suske, M., Vortkamp, A., Bornholdt, D., Konig, R., Grzeschik, K.H., 1997. Point mutations in human GLI3 cause Greig syndrome. Hum. Mol. Genet. 6, 1979–1984.
Zakany, J., Duboule, D., 1999. Hox genes in digit development and evolution. Cell Tissue Res. 296, 19–25.
Zakany, J., Fromental-Ramin, C., Warot, X., Duboule, D., 1997. Regulation of number and size of digits by posterior Hox genes: a dose-dependent mechanisms with potential evolutionary implications. Proc. Natl. Acad. Sci. USA 94, 13695–13700.
Zakany, J., Kmita, M., Duboule, D., 2004. A dual role for Hox genes in limb anterior–posterior asymmetry. Science 304, 1669–1672.